Oberwolfach Preprints

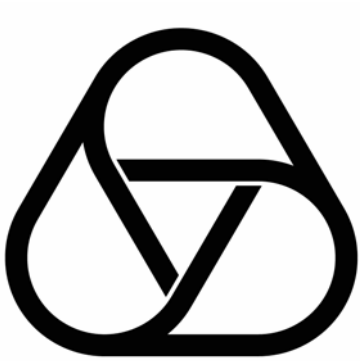

OWP 2013 - 06

HANSJÖRG GEIGES AND SINEM ONARAN

Legendrian Rational Unknots in Lens Spaces

Mathematisches Forschungsinstitut Oberwolfach gGmbH
Oberwolfach Preprints (OWP) ISSN 1864-7596

Oberwolfach Preprints (OWP)

Starting in 2007, the MFO publishes a preprint series which mainly contains research results related to a longer stay in Oberwolfach. In particular, this concerns the Research in Pairs-Programme (RiP) and the Oberwolfach-Leibniz-Fellows (OWLF), but this can also include an Oberwolfach Lecture, for example.

A preprint can have a size from 1 - 200 pages, and the MFO will publish it on its website as well as by hard copy. Every RiP group or Oberwolfach-Leibniz-Fellow may receive on request 30 free hard copies (DIN A4, black and white copy) by surface mail.

Of course, the full copy right is left to the authors. The MFO only needs the right to publish it on its website *www.mfo.de* as a documentation of the research work done at the MFO, which you are accepting by sending us your file.

In case of interest, please send a **pdf file** of your preprint by email to *rip@mfo.de* or *owlf@mfo.de*, respectively. The file should be sent to the MFO within 12 months after your stay as RiP or OWLF at the MFO.

There are no requirements for the format of the preprint, except that the introduction should contain a short appreciation and that the paper size (respectively format) should be DIN A4, "letter" or "article".

On the front page of the hard copies, which contains the logo of the MFO, title and authors, we shall add a running number (20XX - XX).

We cordially invite the researchers within the RiP or OWLF programme to make use of this offer and would like to thank you in advance for your cooperation.

Imprint:

Mathematisches Forschungsinstitut Oberwolfach gGmbH (MFO)
Schwarzwaldstrasse 9-11
77709 Oberwolfach-Walke
Germany

Tel +49 7834 979 50
Fax +49 7834 979 55
Email admin@mfo.de
URL www.mfo.de

The Oberwolfach Preprints (OWP, ISSN 1864-7596) are published by the MFO.

LEGENDRIAN RATIONAL UNKNOTS IN LENS SPACES

HANSJÖRG GEIGES AND SINEM ONARAN

Abstract. We classify Legendrian rational unknots with tight complements in the lens spaces $L(p,1)$ up to coarse equivalence. As an example of the general case, this classification is also worked out for $L(5,2)$. The knots are described explicitly in a contact surgery diagram of the corresponding lens space.

1. Introduction

This paper is concerned with the classification of Legendrian rational unknots in lens spaces. The lens space in question may be equipped with a tight or an overtwisted contact structure, but in the latter case we require that the knot complement be tight. Legendrian knots in overtwisted contact 3-manifolds with tight complement are called *non-loose* or *exceptional*.

The classification of Legendrian unknots in S^3 is due to Eliashberg and Fraser [7]. In the case of the tight standard contact structure ξ_{st} on S^3, their classification is up to isotopy; in the case of exceptional unknots in an overtwisted contact structure, up to coarse equivalence. Recall that two Legendrian knots $L_i \subset (M_i, \xi_i)$, $i = 1, 2$, in contact 3-manifolds are called *coarsely equivalent* if there is a contactomorphism $(M_1, \xi_1) \to (M_2, \xi_2)$ carrying L_1 to L_2. Here the contact structures are understood to be (co-)oriented, and the contactomorphism is supposed to preserve the (co-)orientation. The classification of Legendrian knots in overtwisted contact manifolds up to isotopy is complicated by the fact there are contactomorphisms topologically but not contact isotopic to the identity, cf. the discussion in [7, Section 4.3].

In the present paper we extend the classification result of Eliashberg and Fraser to rational unknots in lens spaces. Our focus will lie on the exceptional case, and we too are content with the classification up to coarse equivalence. The classification in the tight case is essentially due to Baker and Etnyre [1], although they give an explicit description only for $L(p,1)$ with p odd.

We obtain a complete classification (both in the tight and the exceptional case) for the lens spaces $L(p,1)$ with p any integer. As an illustration of the general case we also discuss the classification for $L(5,2)$. In particular, we determine the range of the classical invariants realisable by such rational unknots, and the 3-dimensional homotopy invariant of the contact structures containing exceptional knots.

This classification is achieved as follows. The number of distinct Legendrian rational unknots with tight complements is determined via the classification of tight contact structures on solid tori; this strategy has previously been employed by Etnyre [8]. We then describe the expected number of Legendrian rational unknots explicitly in a contact surgery diagram of the lens space. For the 3-sphere, such a

2010 *Mathematics Subject Classification.* 53D10, 57M25, 57M27.

description is due to Plamenevskaya [17]. In all cases the knots are distinguished by the rational analogues of the classical Legendrian knot invariants.

Here is an outline of the paper. In Section 2 we recall the topological classification of rational unknots in lens spaces. In Section 3 we describe a result of Lisca et al. [14] about the computation of the classical Legendrian knot invariants of a Legendrian knot presented in a contact surgery diagram. We extend their result from integral to rational homology spheres and from nullhomologous to rationally nullhomologous knots. The invariants in this case are the rational Legendrian knot invariants [16, 2, 1].

In Section 4 we recall how to compute the 3-dimensional homotopy invariant of a contact structure from a surgery diagram. This will be used in some cases to show that the contact structure defined by a certain surgery diagram is overtwisted.

Sections 5 to 8 contain the classification for S^3, $\mathbb{R}\mathrm{P}^3$, $L(p,1)$ and $L(5,2)$, respectively. The classification for S^3 and $\mathbb{R}\mathrm{P}^3$ is of course subsumed by that for $L(p,1)$. Nonetheless, the separate description of those two simple cases allows us to include some additional details and to make the whole classification scheme more transparent. Many of the necessary computations are relegated to Section 9.

We understand that Bülent Tosun has been working on the classification problem discussed in this paper using a parallel approach, but staying closer to the argument in [8] rather than relying on surgery diagrams for the existence part of the classification. This may in fact be advantageous for dealing with the general $L(p,q)$.

2. Rational unknots in lens spaces

The lens space $L(p,q)$ with $p \in \mathbb{N}$ and $1 \leq q \leq p-1$ coprime to p is defined as the quotient space of $S^3 \subset \mathbb{C}^2$ under the $\mathbb{Z}_p$-action generated by

$$(z_1, z_2) \longmapsto (\mathrm{e}^{2\pi \mathrm{i}/p} z_1, \mathrm{e}^{2\pi \mathrm{i} q/p} z_2).$$

This gives $L(p,q)$ a canonical orientation, and our contact structures are assumed to be positive for that orientation. Alternatively, $L(p,q)$ with the described orientation can be obtained by surgery along a single $(-p/q)$-framed unknot in S^3.

A *rational unknot* K in some 3-manifold M is a knot with a rational Seifert disc, i.e. some cable of K on the boundary $\partial(\nu K)$ of a tubular neighbourhood of K is supposed to bound a 2-disc D embedded in $M \setminus \nu K$, cf. [1]. As discussed in that paper, the union $\nu K \cup D$ equals the complement of an open ball in a lens space, so for the study of rational unknots one may restrict attention to the case of M being a lens space.

Moreover, a rational unknot[1] in $L(p,q)$ is then necessarily the spine of one of the Heegaard tori. Recall that the genus 1 Heegaard splitting of a lens space is unique up to isotopy [3]. Hence, up to isotopy there are at most four oriented rational unknots in $L(p,q)$, namely $\pm K_j$, $j = 1, 2$, where

$$K_1 = \{[\mathrm{e}^{\mathrm{i}\theta}, 0] \colon\ 0 \leq \theta \leq 2\pi/p\} \subset L(p,q),$$

and likewise for K_2. For $p = 2$ this reduces in fact to one possibility, and for $p > 2$, $q \in \{1, p-1\}$ the knot $\pm K_1$ is isotopic to $\pm K_2$, both being fibres in an S^1-bundle

[1]When we speak of a 'rational unknot' in $L(p,q)$ we always mean a rational unknot that is not an honest unknot, i.e. the homological order of the knot is supposed to be greater than 1.

over S^2. In homology one has $[K_2] = q[K_1]$, so for $q \notin \{1, p-1\}$ there are indeed four rational unknots up to isotopy, see [1, Lemma 5.2].

In the surgery picture, K_1 can be represented as in Figure 1. The knot K_2 would be the spine of the solid torus glued in to perform the surgery. By exchanging the role of the two Heegaard tori, which induces the orientation-preserving diffeomorphism $L(p,q) \cong L(p,r)$ for $qr \equiv 1 \bmod p$, one gets a similar picture for K_2, with the surgery coefficient replaced by $-p/r$.

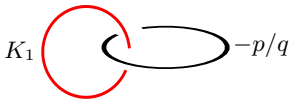

FIGURE 1. One of the rational unknots in $L(p,q)$.

By expanding the rational surgery into integral surgeries along a link of unknots, one can give representations of K_1 and K_2 in a single surgery diagram. For instance, in the case $p = 5$, $q = 2$ we can take $r = 3$. Since $-5/2 = -3 - 1/(-2)$ and $-5/3 = -2 - 1/(-3)$ we can represent K_1 and K_2 as in Figure 2. A slam dunk, cf. [12, Figure 5.30], will then produce Figure 1 or the analogous picture for K_2, respectively.

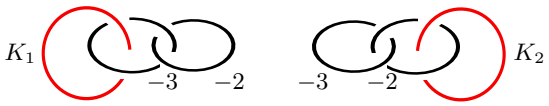

FIGURE 2. The two rational unknots in $L(5,2)$.

Since we are interested in a classification up to coarse equivalence, we need to take the action of the diffeomorphism group into account. In this topological setting, coarse equivalence of two knots is supposed to mean that there is an orientation-preserving diffeomorphism of the ambient manifold sending one knot to the other.

Proposition 1. *Up to coarse equivalence there is exactly one oriented rational unknot in $L(p,q)$ for $q^2 \equiv 1 \bmod p$, and exactly two for $q^2 \not\equiv 1 \bmod p$.*

Proof. The orientation-preserving diffeomorphism of $L(p,q)$ induced by $(z_1, z_2) \mapsto (\overline{z}_1, \overline{z}_2)$ sends K_j to $-K_j$, $j = 1, 2$. Thus, topologically we can ignore the orientation of K_j.

For $q^2 \equiv 1 \bmod p$, the orientation-preserving diffeomorphism of $L(p,q)$ induced by $(z_1, z_2) \mapsto (z_2, z_1)$ exchanges K_1 and K_2. For $q^2 \not\equiv 1 \bmod p$, there are only two orientation-preserving diffeomorphisms of $L(p,q)$ up to isotopy: the identity and the one described above, see [15]. So K_1 and K_2 cannot be coarsely equivalent. □

However, as pointed out in [1] for the tight case, the two different orientations of K_1 may correspond to non-equivalent Legendrian realisations. Similar considerations apply in the exceptional case. This gives some information about the contactomorphism group of the corresponding contact structure.

3. The classical invariants

In this section we first recall from [1] how to define the classical invariants for *rationally* nullhomologous Legendrian knots. We then show how to compute these invariants for knots presented in a surgery diagram of the ambient manifold, provided this manifold is a rational homology sphere. This constitutes a mild extension of a result due to Lisca et al. [14, Lemma 6.6].

3.1. **Definition of the invariants.** Let $L \subset (Y,\xi)$ be a rationally nullhomologous Legendrian knot in a contact 3-manifold, i.e. L is of some order $r \in \mathbb{N}$ in $H_1(Y)$. Then there is a rational Seifert surface $\Sigma \subset Y$ for rL, i.e. a surface that is embedded, except along its boundary, which is an r-fold covering of L. Note that the boundary of Σ need not be connected. (One can replace L by a suitable embedded curve or collection of curves on the boundary of a tubular neighbourhood of L, representing the class rL in the tubular neighbourhood, and then find an embedded surface with that curve (or those curves) as its boundary.) Let L' be a push-off of L in the direction of the contact framing, i.e. the framing determined by $\xi|_L$. Then the *rational Thurston–Bennequin invariant* of L is

$$\mathtt{tb}_{\mathbb{Q}}(L) := \frac{1}{r} L' \bullet \Sigma,$$

i.e. the rational linking number of L and L'. Any two rational Seifert surfaces for L differ by a class in $H_2(Y)$. Since L' is rationally nullhomologous, its intersection number with such a class is zero, so $\mathtt{tb}_{\mathbb{Q}}(L)$ is well defined.

Now assume that L is oriented. The contact structure ξ is a trivial plane bundle when restricted to the rational Seifert surface Σ, and the *rational rotation number* $\mathtt{rot}_{\mathbb{Q}}(L)$ is defined by writing $r\cdot\mathtt{rot}_{\mathbb{Q}}(L)$ for the number of full turns of the positive tangent vector to L, as L is traversed r times, relative to the trivialisation of $\xi|_\Sigma$. In general, this number will depend on the relative homology class represented by Σ. If the Euler class $e(\xi)$ is a torsion class, then $\mathtt{rot}_{\mathbb{Q}}(L)$ is well defined.

3.2. **Computation in a surgery diagram.** As shown in [4], any (closed, connected) contact 3-manifold (Y,ξ) has a contact (±1)-surgery presentation $\mathbb{L} = \mathbb{L}_+ \sqcup \mathbb{L}_- \subset (S^3,\xi_{\mathrm{st}})$, i.e. there is a Legendrian link $\mathbb{L}$ in S^3 with its standard tight contact structure such that contact (±1)-surgery along the components of $\mathbb{L}_\pm$ produces (Y,ξ).

Now let $\mathbb{L} = \mathbb{L}_+ \sqcup \mathbb{L}_-$ be a contact (±1)-surgery presentation of a rational homology 3-sphere (Y,ξ). Then $H^2(Y)$ will be a finite abelian group, so the Euler class $e(\xi)$ is a torsion class. Furthermore, let $L_0 \subset (S^3\setminus\mathbb{L},\xi_{\mathrm{st}})$ be a Legendrian knot that becomes rationally nullhomologous in (Y,ξ). Denote the link components of $\mathbb{L}$ by $L_1,\dots,L_n$, and set $a_i = \mathtt{tb}(L_i) \pm 1$, depending on whether L_i belongs to $\mathbb{L}_+$ or $\mathbb{L}_-$. So a_i is the integral surgery coefficient of the link component L_i. Write M for the linking matrix of $\mathbb{L}$, i.e.

$$M := (m_{ij})_{i,j=1}^n, \quad \text{where } m_{ij} := \begin{cases} a_i & \text{if } i=j,\\ \mathtt{lk}(L_i,L_j) & \text{if } i\neq j.\end{cases}$$

Define an extended matrix by

$$M_0 := (m_{ij})_{i,j=0}^n, \quad \text{where } m_{ij} := \begin{cases} 0 & \text{if } i=j=0,\\ a_i & \text{if } i=j\neq 0,\\ \mathtt{lk}(L_i,L_j) & \text{if } i\neq j.\end{cases}$$

In other words, M_0 is the linking matrix of $L_0 \sqcup \mathbb{L}$, with the convention that $\mathtt{lk}(L_0, L_0)$ is set to 0. As a final piece of notation, we write $\mathtt{rot}_i$ for the rotation number of L_i, $i = 0, \dots, n$, and $\mathtt{tb}_0$ for the Thurston–Bennequin invariant of L_0, all regarded as knots in (S^3, ξ_{st}).

We can now formulate a lemma that tells us how to compute the classical invariants of L_0 when it is regarded as a Legendrian knot in the surgered manifold (Y, ξ). For the case that (Y, ξ) is an integral homology sphere, this lemma is due to Lisca et al. [14, Lemma 6.6]. (The condition that Y be an integral homology sphere is not contained in the statement of their lemma, but in the paragraphs preceding it, and it is used implicitly in their argument.)

Lemma 2. *The rational invariants of $L_0 \subset (Y, \xi)$ are given by*

$$\mathtt{rot}_{\mathbb{Q}}(L_0) = \mathtt{rot}_0 - \left\langle \begin{pmatrix} \mathtt{rot}_1 \\ \vdots \\ \mathtt{rot}_n \end{pmatrix}, M^{-1} \begin{pmatrix} \mathtt{lk}(L_0, L_1) \\ \vdots \\ \mathtt{lk}(L_0, L_n) \end{pmatrix} \right\rangle$$

and

$$\mathtt{tb}_{\mathbb{Q}}(L_0) = \mathtt{tb}_0 + \frac{\det M_0}{\det M}.$$

These formulae are exactly the same as those in [14], with $\mathtt{tb}$ and $\mathtt{rot}$ replaced by their rational counterparts. However, since it is not entirely clear where the order of L in $H_1(Y)$ might or might not be relevant for the argument, we deem it worth to include a proof.

3.3. **The relative Euler class.** Before we turn to that proof, we want to discuss the behaviour of the relative Euler class of a contact structure under a contact (± 1)-surgery along a Legendrian knot L_i. A neighbourhood of L_i can be identified with a neighbourhood of $S^1 \times \{0\} \subset S^1 \times \mathbb{R}^2$, equipped with the contact structure $\ker(\cos\theta\, dx - \sin\theta\, dy)$. We think of $S^1 \times D^2 \subset S^1 \times \mathbb{R}^2$ as the solid torus we cut out during the surgery. The boundary $S^1 \times \partial D^2$ of this solid torus is a convex surface with two dividing curves $(\pm\sin\theta, \pm\cos\theta, \theta)$. These curves lie in the class of the longitude λ_{c} giving the contact framing. Write μ for the meridian of $S^1 \times \partial D^2$ and λ for the standard longitude $S^1 \times \{*\}$. Then $\lambda_{\mathrm{c}} = \lambda - \mu$. Thus, in terms of the standard meridian and longitude μ, λ, the slope of the dividing curves is -1. The convex torus $S^1 \times \partial D^2$ has a linear Legendrian ruling given by the θ-curves, which represent the class $\lambda = \mu + \lambda_{\mathrm{c}}$.

Write μ', λ' for meridian and longitude, respectively, of a solid torus we glue in to perform the surgery. Contact (-1)-surgery can be described by the gluing maps

$$\mu' \longmapsto \mu - \lambda_{\mathrm{c}}, \quad \lambda' \longmapsto \mu;$$

contact $(+1)$-surgery, by the maps

$$\mu' \longmapsto \mu + \lambda_{\mathrm{c}}, \quad \lambda' \longmapsto \mu + 2\lambda_{\mathrm{c}}.$$

Note that in both cases $\lambda' - \mu'$ gets glued to λ_{c}. So the slope of the dividing curves on the boundary of the solid torus we want to glue in is again -1, now with respect to μ', λ'.

The Legendrian ruling of the convex torus $S^1 \times \partial D^2$ in the original model can be changed from the class $\lambda = \lambda_{\mathrm{c}} + \mu$ to either μ or $\mu + 2\lambda_{\mathrm{c}}$ by an isotopic deformation of the 2-torus through convex tori of slope -1 and linear Legendrian ruling, staying

inside any arbitrarily small neighbourhood of the original torus. After this modification, we see that contact (± 1)-surgery simply corresponds to regluing a standard solid torus with slope -1 and linear Legendrian ruling in the class λ_0.

Now suppose that we perform contact (± 1)-surgery along a Legendrian knot L in a contact 3-manifold (M, ξ_0). The relative Euler class $e(\xi_0, L) \in H^2(M, L)$ is Poincaré dual to the class in $H_1(M \setminus L)$ represented by the zero set of a generic section of ξ_0 that coincides with the tangent direction along L. By what we just discussed, we may assume that this section coincides with the Legendrian ruling on the boundary of a standard tubular neighbourhood of L, and this section will extend without zeros over the solid torus we glue in when performing a surgery along L. Translated into our situation at hand, this implies the following statement.

Lemma 3. *Under the natural map*

$$H_1(S^3 \setminus (L_0 \sqcup \ldots \sqcup L_n)) \longrightarrow H_1(Y \setminus L_0)$$

induced by inclusion, the Poincaré dual of the relative Euler class $e(\xi_{\mathrm{st}}, L_0 \sqcup \ldots \sqcup L_n)$ maps to the Poincaré dual of $e(\xi, L_0)$. □

3.4. **Proof of Lemma 2.** Write μ_i for the meridian of L_i, and λ_i for the longitude determined by the surface framing. Then

$$H_1(S^3 \setminus \bigsqcup_{i=0}^{n} L_i) \cong \mathbb{Z}_{\mu_0} \oplus \cdots \oplus \mathbb{Z}_{\mu_n},$$

where $\mathbb{Z}_\mu$ denotes a copy of the integers generated by the class μ. In $S^3 \setminus \bigsqcup_{i=0}^{n} L_i$, the longitude λ_i represents the class

$$\lambda_i = \sum_{\substack{j=0 \\ j \neq i}}^{n} \mathtt{lk}(L_i, L_j)\mu_j. \tag{1}$$

Surgery with coefficient a_i along L_i means that we glue a new meridional disc along $a_i\mu_i + \lambda_i$, $i = 1, \ldots, n$. It follows that

$$H_1(Y \setminus L_0) \cong \mathbb{Z}_{\mu_0} \oplus \cdots \oplus \mathbb{Z}_{\mu_n} / \langle a_i\mu_i + \sum_{\substack{j=0 \\ j \neq i}}^{n} \mathtt{lk}(L_i, L_j)\mu_j = 0,\ i = 1, \ldots, n \rangle.$$

On the other hand, from the Mayer–Vietoris sequence of the triple $(Y; Y \setminus L_0, L_0)$ and the assumption that Y be a rational homology sphere (as well as some obvious identifications under excision isomorphisms) we have the short exact sequence

$$0 \longrightarrow H_1(T^2) \longrightarrow H_1(Y \setminus L_0) \oplus H_1(L_0) \longrightarrow H_1(Y) \longrightarrow 0,$$

with $H_1(Y)$ a finite abelian group. We have $H_1(T^2) \cong \mathbb{Z}_{\mu_0} \oplus \mathbb{Z}_{\lambda_0}$. The class μ_0 maps to 0 in $H_1(L_0) \cong \mathbb{Z}$; the class λ_0, to 1. So the sequence reduces to

$$0 \longrightarrow \mathbb{Z}_{\mu_0} \longrightarrow H_1(Y \setminus L_0) \longrightarrow H_1(Y) \longrightarrow 0. \tag{2}$$

(Alternatively, this follows from L_0 being rationally nullhomologous in Y.)

Hence the Poincaré dual of the relative Euler class $e(\xi, L_0)$ over the rationals,

$$\mathrm{PD}(e(\xi, L_0))_{\mathbb{Q}} := \mathrm{PD}(e(\xi, L_0)) \otimes_{\mathbb{Z}} 1 \in H_1(Y \setminus L_0; \mathbb{Q}) \cong \mathbb{Q}_{\mu_0},$$

is some rational multiple of μ_0. Beware that — over the integers — μ_0 is not, in general, a primitive element in $H_1(Y \setminus L_0)$. For instance, for $Y = \mathbb{R}\mathrm{P}^3$ and L_0

representing the generator of $\pi_1(\mathbb{R}\mathrm{P}^3) = \mathbb{Z}_2$, the class μ_0 is twice the generator of $H_1(\mathbb{R}\mathrm{P}^3 \setminus L_0) \cong \mathbb{Z}$.

The definition of the rotation number of a Legendrian knot can be interpreted in terms of relative Euler classes. This translates into

$$\mathrm{PD}\big(e(\xi_{\mathrm{st}}, \bigsqcup_{i=0}^{n} L_i)\big) = \sum_{i=0}^{n} \mathtt{rot}_i \mu_i.$$

For the rational rotation number $\mathtt{rot}_{\mathbb{Q}}(L_0)$ of $L_0 \subset (Y, \xi)$ we argue similarly. If the order of L_0 in $H_1(Y)$ is r, and Σ is a rational Seifert surface for L_0 in Y, then

$$r \cdot \mathtt{rot}_{\mathbb{Q}}(L_0) = \langle e(\xi, L_0), [\Sigma] \rangle = \mathrm{PD}(e(\xi, L_0)) \bullet \Sigma.$$

For this intersection product, only the free part of $\mathrm{PD}(e(\xi, L_0))$ is relevant, and since the intersection product $\mu_0 \bullet [\Sigma]$ equals r, we conclude that

$$\mathrm{PD}(e(\xi, L_0))_{\mathbb{Q}} = \mathtt{rot}_{\mathbb{Q}}(L_0)\mu_0.$$

Hence, by Lemma 3,

$$\sum_{i=0}^{n} \mathtt{rot}_i \mu_i = \mathtt{rot}_{\mathbb{Q}}(L_0)\mu_0 \text{ in } H_1(Y \setminus L_0; \mathbb{Q}).$$

The relations in the presentation of $H_1(Y \setminus L_0)$ can be written formally as

$$M \begin{pmatrix} \mu_1 \\ \vdots \\ \mu_n \end{pmatrix} + \begin{pmatrix} \mathtt{lk}(L_0, L_1) \\ \vdots \\ \mathtt{lk}(L_0, L_n) \end{pmatrix} \mu_0 = 0.$$

The surgery description of Y defines a 4-dimensional handlebody X with boundary $\partial X = Y$. Both $H_2(X)$ and $H_2(X, Y)$ are isomorphic to $\mathbb{Z}^n$. The relevant part of the homology exact sequence of the pair (X, Y) is

$$H_2(Y) \longrightarrow H_2(X) \xrightarrow{M} H_2(X, Y) \longrightarrow H_1(Y).$$

Since Y is a rational homology sphere, we have $H_2(Y) = 0$, so the matrix M is invertible over $\mathbb{Q}$. Therefore, in $H_1(Y \setminus L_0; \mathbb{Q})$ we have

$$\mathtt{rot}_{\mathbb{Q}}(L_0)\mu_0 = \sum_{i=0}^{n} \mathtt{rot}_i \mu_i = \Big(\mathtt{rot}_0 - \Big\langle \begin{pmatrix} \mathtt{rot}_1 \\ \vdots \\ \mathtt{rot}_n \end{pmatrix}, M^{-1} \begin{pmatrix} \mathtt{lk}(L_0, L_1) \\ \vdots \\ \mathtt{lk}(L_0, L_n) \end{pmatrix} \Big\rangle\Big)\mu_0.$$

This proves the first formula in the lemma.

We now turn to the Thurston–Bennequin invariant. The contact framing of L_0 (both in (S^3, ξ_{st}) and in (Y, ξ)) is given by $\mathtt{tb}_0\mu_0 + \lambda_0$. On the other hand, from the exact sequence (2) we see that there is a unique $a_0 \in \mathbb{Z}$ such that $a_0\mu_0 + r\lambda_0$ is nullhomologous in $Y \setminus L_0$, where as before r denotes the order of L_0 in Y. Then the rational Thurston–Bennequin invariant of L_0 in (Y, ξ) can be computed as

$$r \cdot \mathtt{tb}_{\mathbb{Q}}(L_0) = (\mathtt{tb}_0\mu_0 + \lambda_0) \bullet (a_0\mu_0 + r\lambda_0) = r \cdot \mathtt{tb}_0 - a_0, \tag{3}$$

where the intersection product should be interpreted as a product on the boundary of a tubular neighbourhood of L_0.

From (1) we have

$$a_0\mu_0 + r\lambda_0 = a_0\mu_0 + r\sum_{j=1}^{n} \mathtt{lk}(L_0, L_j)\mu_j,$$

and the fact that this is nullhomologous in $Y \setminus L_0$ means that it can be expressed as a linear combination of the relations in $H_1(Y \setminus L_0)$, which yields

$$0 = \begin{vmatrix} a_0 & r \cdot \mathtt{lk}(L_0, L_1) & \cdots & r \cdot \mathtt{lk}(L_0, L_n) \\ \mathtt{lk}(L_1, L_0) & a_1 & \cdots & \mathtt{lk}(L_1, L_n) \\ \vdots & \vdots & \ddots & \vdots \\ \mathtt{lk}(L_n, L_0) & \mathtt{lk}(L_n, L_1) & \cdots & a_n \end{vmatrix} = a_0 \det M + r \det M_0.$$

With (3) we get

$$\mathtt{tb}_{\mathbb{Q}}(L) = \mathtt{tb}_0 - \frac{a_0}{r} = \mathtt{tb}_0 + \frac{\det M_0}{\det M}.$$

4. Invariants of tangent 2-plane fields

A surgery presentation $\mathbb{L} = \mathbb{L}_+ \sqcup \mathbb{L}_- \subset (S^3, \xi_{\mathrm{st}})$ of a given contact 3-manifold (Y, ξ) determines a 4-dimensional 2-handlebody X with boundary $\partial X = Y$. Following [11] and [5] we are now going to explain how to determine the homotopical data of ξ as a tangent 2-plane field from such a presentation.

Given a choice of spin structure s on Y, there is an invariant $\Gamma(\xi, s) \in H_1(Y)$ of the homotopy type of ξ over the 2-skeleton of Y. When the first Chern class $c_1(\xi)$ is a torsion class, the homotopy obstruction over the 3-skeleton can be described by a rational number $d_3(\xi)$.

In [11, Theorem 4.12] it is shown how to compute $\Gamma(\xi, s)$ from a surgery diagram containing only contact (-1)-surgeries. A spin structure s can be specified in terms of a characteristic sublink in the surgery diagram. Bülent Tosun has informed us of a way to compute the 2-dimensional homotopy invariant $\Gamma(\xi, s)$ from any contact surgery diagram, including those with 1-handles and contact $(+1)$-surgeries. This would allow one to give a complete homotopy classification of the contact structures on $L(p, q)$ we describe in terms of surgery diagrams in the following sections.

The 3-dimensional invariant can be computed as follows. Write $\sigma(X)$ for the signature of X, and $\chi(X)$ for its Euler characteristic. Let $\Sigma_i \subset X$ be the surface obtained by gluing a Seifert surface of L_i with the core disc of the handle corresponding to $L_i \subset \mathbb{L}$. The homology class of Σ_i in $H_2(X)$ is completely determined by $L_i \subset S^3$. Generalising a result of Gompf, the following was shown in [5].

Proposition 4. *Suppose that $c_1(\xi)$ is torsion, and $\mathtt{tb}(L_i) \neq 0$ for each $L_i \in \mathbb{L}_+$. Then*

$$d_3(\xi) = \frac{1}{4}\big(c^2 - 3\sigma(X) - 2\chi(X)\big) + q, \tag{4}$$

where q denotes the number of components of $\mathbb{L}_+$, and $c \in H^2(X)$ is the cohomology class determined by $c(\Sigma_i) = \mathtt{rot}(L_i)$ for each $L_i \subset \mathbb{L}$.

See [5] of an extensive discussion of this formula, in particular concerning the computation of the term c^2.

The standard (and unique tight) contact structure ξ_{st} on S^3 has $d_3(\xi_{\mathrm{st}}) = -1/2$. On $L(p, 1)$ there are, by [10] and [13], exactly $p - 1$ tight contact structures up to isotopy. They can be obtained by contact (-1)-surgery on S^3 along a single unknot with invariants $\mathtt{tb} = -p + 1$ and

$$\mathtt{rot} \in \{-p + 2, -p + 4, \ldots, p - 4, p - 2\},$$

obtained from the standard Legendrian unknot ($\mathtt{tb} = -1, \mathtt{rot} = 0$) by any mix of $p-2$ positive or negative stabilisations. The d_3-invariant of the corresponding contact structure on $L(p,1)$ is given by

$$d_3 = -\frac{1}{4}\big(1 + \frac{\mathtt{rot}^2}{p}\big).$$

5. The 3-sphere

Topologically trivial Legendrian knots in arbitrary tight contact 3-manifolds were shown by Eliashberg and Fraser [7] to be classified up to Legendrian isotopy by the classical invariants $\mathtt{tb}$ and $\mathtt{rot}$, and they determined the range of these invariants. So part (a) of the following theorem is a weaker formulation of their result, which we include for completeness and comparison with the case of exceptional knots.

The exceptional unknots in the 3-sphere S^3 have also been classified, up to coarse equivalence, by Eliashberg and Fraser [7, Theorem 4.7]. An alternative proof of their result was given by Etnyre and Vogel, see [8]. We are going to give yet another proof of this classification, which contains *in nuce* all the key ideas required to extend the result to lens spaces. Our argument for determining an upper bound on the number of exceptional knots is parallel to that of [8]. The proof is then completed by finding as many explicit realisations of exceptional unknots as this bound allows. In the case of S^3, these explicit realisations are due to Plamenevskaya [17].

Theorem 5 (Eliashberg–Fraser)**.** (a) *Let $L \subset (S^3, \xi_{\mathrm{st}})$ be a Legendrian unknot. Then $\mathtt{tb}(L) = n$ with n a negative integer, and $\mathtt{rot}(L)$ lies in the range*

$$\{n+1, n+3, \dots, -n-3, -n-1\}.$$

Any such pair of invariants $(\mathtt{tb}, \mathtt{rot})$ is realised, and it determines L up to coarse equivalence, i.e. for each $n \le -1$ we have $|n|$ distinct Legendrian unknots.

(b) *Let $L \subset (S^3, \xi)$ be an exceptional unknot in an overtwisted contact structure ξ on S^3. Then ξ is the contact structure determined up to isotopy by $d_3(\xi) = 1/2$, and*

$$\big(\mathtt{tb}(L), \mathtt{rot}(L)\big) \in \big\{(n, \pm(n-1)) \colon\ n \in \mathbb{N}\big\}.$$

These invariants determine L up to coarse equivalence, and any pair of invariants in this set is realised.

Proof. Examples of Legendrian unknots in (S^3, ξ_{st}) that realise the invariants stated in the theorem are given by arbitrary stabilisations of a standard Legendrian unknot with $\mathtt{tb} = -1$ and $\mathtt{rot} = 0$.

Examples of exceptional unknots with the stated invariants have been described by Plamenevskaya [17] in terms of the front projection of the knot in a contact surgery diagram, see Figure 3.

Each of these diagrams gives a copy of S^3, as can be seen by simple Kirby moves, cf. [17]. A straightforward computation with the formula from Proposition 4 shows that each diagram gives a contact structure on S^3 with $d_3 = 1/2$. So this contact structure is overtwisted (and determined up to isotopy by this value of d_3 thanks to Eliashberg's classification of overtwisted contact structures [6], cf. [9]). Contact (-1)-surgery along L cancels the $(+1)$-surgery along the parallel knot, see [4, Section 3] or [9, Prop. 6.4.5]. This leaves us with a diagram containing only contact (-1)-surgeries, or one with a single $(+1)$-surgery along the standard Legendrian unknot. The latter produces the tight contact structure on $S^1 \times S^2$,

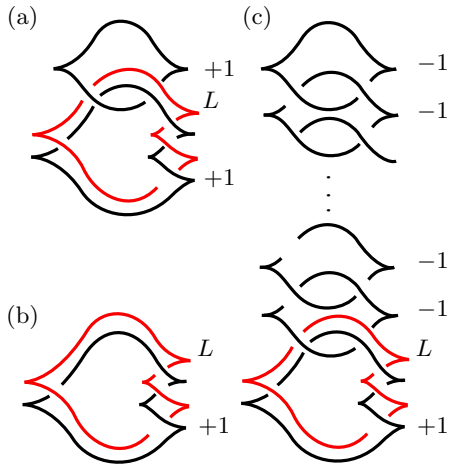

FIGURE 3. The exceptional unknots in the 3-sphere.

see [5, Lemma 4.3], the former a Stein fillable and hence tight contact structure. This shows that in all examples the knot L is exceptional.

We claim that the knot L in Figure 3(a) has $(\mathtt{tb}, \mathtt{rot}) = (1, 0)$, the one in (b) has $(\mathtt{tb}, \mathtt{rot}) = (2, \pm 1)$ (depending on a choice of orientation of L), and the one in (c) (with $n - 2 \geq 1$ unknots along which we perform (-1)-surgery) has $(\mathtt{tb}, \mathtt{rot}) = (n, \pm(n-1))$.

Plamenevskaya determines $\mathtt{tb}(L)$ by keeping track of the contact framing through Kirby moves; no comment is made about $\mathtt{rot}(L)$. In fact, the claimed values of $\mathtt{tb}(L)$ and $\mathtt{rot}(L)$ follow easily from Lemma 2. See Section 9 for some details of these computations.

So we are left with showing that these invariants (in the tight and exceptional case, respectively) determine L up to coarse equivalence, and that no other values of the classical invariants can be realised.

Given a Legendrian unknot L in (S^3, ξ_{st}) or an exceptional unknot L in S^3, decompose the 3-sphere along a torus as $S^3 = V_1 \cup V_2$, with V_1 a standard neighbourhood of L. More precisely, with μ_i, λ_i denoting meridian and longitude of the solid tori V_i, we assume that the gluing is described by the identifications $\mu_1 = \lambda_2$, $\lambda_1 = \mu_2$, and ∂V_1 is a convex torus with two dividing curves of slope $1/n$, where $n := \mathtt{tb}(L)$.

Both in the tight and the exceptional case, the contact structure on V_2 is tight, and the boundary ∂V_2 is convex with two dividing curves of slope n. Moreover, up to coarse equivalence L is determined by the contact structure on V_2. According to Giroux [10] and Honda [13], the number of tight contact structures on a solid torus V inducing a fixed characteristic foliation on ∂V divided by two curves of slope $-p/q < -1$ is given by

$$|(r_0 + 1) \cdot \ldots \cdot (r_{k-1} + 1) \cdot r_k|,$$

where the $r_i < -1$ are the terms in the continued fraction expansion

$$-\frac{p}{q} = r_0 - \cfrac{1}{r_1 - \cfrac{1}{r_2 - \cdots - \cfrac{1}{r_k}}} =: [r_0, \ldots, r_k];$$

for slope -1 there is a unique structure.

For $n < 0$ the continued fraction expansion is given by $k = 0$ and $r_0 = n$, i.e. we have $|n|$ distinct tight structures, which corresponds to the $|n|$ realisations of a Legendrian unknot with $\mathtt{tb} = n$ in (S^3, ξ_{st}) described above.

For $n = 0$, the contact structure on V_2 would have to be overtwisted, so this case does not occur in (S^3, ξ_{st}) or when L is exceptional.

Finally, for $n > 0$ we first have to modify V_2 by a Dehn twist such that the dividing curves have a slope ≤ -1, in order to apply the classification result cited above. A Dehn twist of V_2 that replaces λ_2 by $\lambda_2' = \lambda_2 + k\mu_2$ changes the slope to $s_2' = n/(1 - kn)$, since

$$\mu_2 + n\lambda_2 = (1 - kn)\mu_2 + n\lambda_2'.$$

For $n = 1$ we have to take $k = 2$, which gives $s_2' = -1$. For this slope there is exactly one tight contact structure on V_2. For $n \geq 2$, we have to take $k = 1$, resulting in a slope $s_2' = -n/(n-1)$. In this case there are exactly two tight contact structures on V_2, for inductively one sees that the continued fraction expansion of $-n/(n-1)$ is $[-2, \ldots, -2]$.

Thus, for $n \geq 1$ the number of tight contact structures on V_2 equals the number of examples in Figure 3. It follows that these examples constitute a complete list of exceptional unknots. □

6. Projective space

The following is the analogue of Theorem 5 for the real projective space $\mathbb{R}\mathrm{P}^3 = L(2,1)$.

Theorem 6. (a) *Let $L \subset (\mathbb{R}\mathrm{P}^3, \xi_{\mathrm{st}})$ be a Legendrian rational unknot in the unique tight contact structure on $\mathbb{R}\mathrm{P}^3$. Then $\mathtt{tb}_{\mathbb{Q}}(L) = n + 1/2$ with n a negative integer, and $\mathtt{rot}_{\mathbb{Q}}(L)$ lies in the range*

$$\{n+1, n+3, \ldots, -n-3, -n-1\}.$$

Any such pair of invariants $(\mathtt{tb}_{\mathbb{Q}}, \mathtt{rot}_{\mathbb{Q}})$ is realised, and it determines L up to coarse equivalence, i.e. for each $n \leq -1$ we have $|n|$ distinct Legendrian rational unknots.

(b) *Up to coarse equivalence, the exceptional rational unknots L in an overtwisted $(\mathbb{R}\mathrm{P}^3, \xi)$ are in one-to-one correspondence with the following set of values of the classical invariants:*

$$\big(\mathtt{tb}_{\mathbb{Q}}(L), \mathtt{rot}_{\mathbb{Q}}(L)\big) \in \big\{(n + 1/2, \pm n),\ (m + 1/2, \pm(m-1))\colon\ n \in \mathbb{N}_0,\ m \in \mathbb{N}\big\}.$$

The overtwisted contact structure containing the knots of the first series has d_3-invariant equal to $1/4$, the one containing the second series has $d_3 = 3/4$.

In other words, there is exactly one exceptional rational unknot with $\mathtt{tb} = 1/2$, there are three with $\mathtt{tb} = 3/2$, and there are four each for $\mathtt{tb} = (2n+1)/2$ with $n \geq 2$.

Proof. Legendrian rational unknots in $(\mathbb{R}\mathrm{P}^3, \xi_{\mathrm{st}})$ that realise the stated values of the invariants are given as follows. Represent $(\mathbb{R}\mathrm{P}_3, \xi_{\mathrm{st}})$ by (-1)-surgery along a single standard Legendrian unknot in S^3 with $\mathtt{tb} = -1$ and $\mathtt{rot} = 0$, and let L_0 be a push-off of the surgery curve with $k-1$ positive and $|n|-k$ negative stabilisations, $k = 1, \ldots, |n|$. Observe that by Lemma 2 the push-off without any stabilisations has $\mathtt{tb}_{\mathbb{Q}} = -1 + \frac{-1}{-2} = -1/2$.

Examples of exceptional rational unknots with the stated invariants are shown in Figures 4 and 5. With some simple Kirby moves one sees that in all cases L is an isotopic copy of the standard rational unknot $L_0 \subset \mathbb{R}\mathrm{P}^3$. We illustrate this in Section 9 for the example in Figure 5(a); there we also explain how $\mathtt{tb}_{\mathbb{Q}}(L)$ can be computed from such Kirby moves instead of Lemma 2.

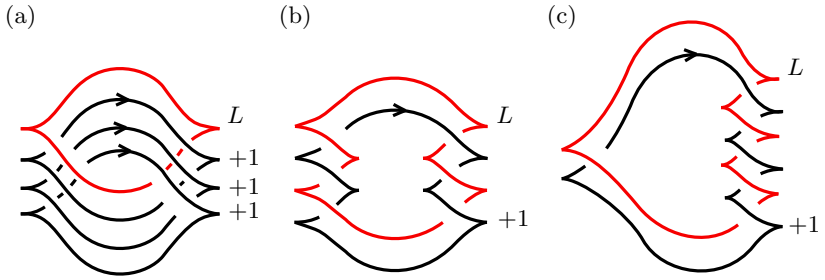

FIGURE 4. Exceptional rational unknots in projective 3-space I.

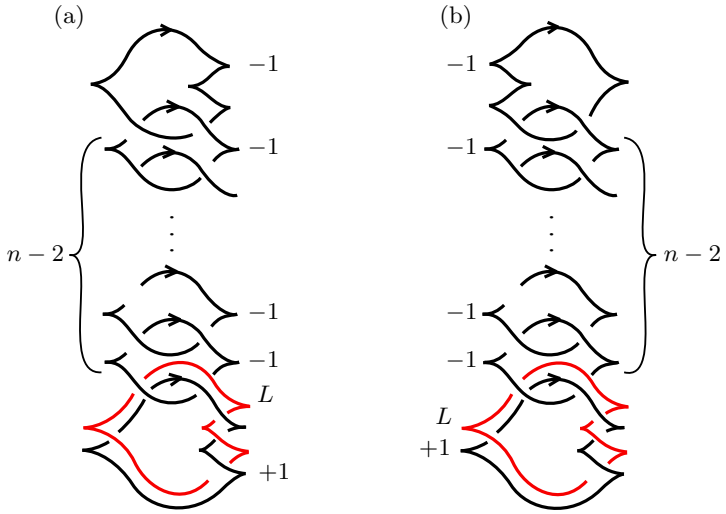

FIGURE 5. Exceptional rational unknots in projective 3-space II.

The invariants of these exceptional examples are listed in Table 1. A sample computation of these invariants is given in Section 9. Since the d_3-invariant differs from $d_3(\xi_{\mathrm{st}}) = -1/4$, all contact structures given by these surgery diagrams are overtwisted.

Figure	n	$\mathtt{tb}_{\mathbb{Q}}(L)$	$\mathtt{rot}_{\mathbb{Q}}(L)$	$d_3(\xi)$
4(a)	-	$1/2$	0	$1/4$
4(b)	-	$3/2$	0	$3/4$
4(c)	-	$3/2$	± 1	$1/4$
5(a)	even ≥ 2	$n+1/2$	$\pm(n-1)$	$3/4$
5(b)	odd ≥ 3	$n+1/2$	$\pm(n-1)$	$3/4$
5(a)	odd ≥ 3	$n+1/2$	$\pm n$	$1/4$
5(b)	even ≥ 2	$n+1/2$	$\pm n$	$1/4$

TABLE 1. Invariants of the exceptional rational unknots in $\mathbb{R}\mathrm{P}^3$.

Except for the example in Figure 4(a), a single contact (-1)-surgery along L produces a Stein fillable contact manifold. In that first example, contact (-1)-surgery along L and two push-offs of L, which by the algorithm in [5] is equivalent to contact $(-1/3)$-surgery along L, yields (S^3, ξ_{st}). So in all cases L is exceptional.

By a similar argument as in the proof of Theorem 5 we are now going to show that this amounts to a complete list of the rational unknots in $\mathbb{R}\mathrm{P}^3$ up to coarse equivalence. Given a Legendrian rational unknot L in $(\mathbb{R}\mathrm{P}^3, \xi_{\mathrm{st}})$ or an exceptional rational unknot L in $\mathbb{R}\mathrm{P}^3$, we decompose $\mathbb{R}\mathrm{P}^3$ into two solid tori V_1, V_2, with V_1 a standard neighbourhood of L. From the standard surgery picture in Figure 1 we see that the gluing of V_1 and V_2 is given by $\mu_2 = -\mu_1 + 2\lambda_1$ and $\lambda_2 = \lambda_1$. Suppose the contact framing of L is $\lambda_{\mathrm{c}} = n\mu_1 + \lambda_1$ for some $n \in \mathbb{Z}$. Then

$$\lambda_{\mathrm{c}} \bullet \mu_2 = (n\mu_1 + \lambda_1) \bullet (-\mu_1 + 2\lambda_1) = 2n + 1,$$

hence $\mathtt{tb}_{\mathbb{Q}}(L) = n + 1/2$.

In order to compute the slope of the convex torus ∂V_2, we need to express λ_c in terms of μ_2 and λ_2:

$$\lambda_{\mathrm{c}} = n\mu_1 + \lambda_1 = -n\mu_2 + (2n+1)\lambda_2.$$

So the slope is $s_2 = -2 - 1/n$.

For $n \leq -1$ the result of Giroux and Honda quoted in the proof of Theorem 5 tells us that there are $|n|$ distinct tight contact structures on V_2. These are all realised as the complement of a rational unknot L_0 in the tight $(\mathbb{R}\mathrm{P}_3, \xi_{\mathrm{st}})$ with $\mathtt{tb}_{\mathbb{Q}}(L_0) = n + 1/2$.

For $n = 0$ the slope s_2 is infinite. This can be changed to -1 by a single Dehn twist. So there is a unique tight contact structure on V_2. For $n \geq 1$, it is easy to see inductively that the slope $s_2 = -2 - 1/n$ has the continued fraction expansion $[-3, -2, \ldots, -2]$, where -2 occurs $n-1$ times. So, by Giroux and Honda, there are three tight structures for $n = 1$, and four each for $n \geq 2$. In all cases, this equals the number of examples in Figures 4 and 5. □

7. The lens spaces $L(p, 1)$

The discussion of the preceding section easily generalises to the lens spaces $L(p, 1)$. The following theorem subsumes Theorems 5 and 6. Part (a) is essentially the same as [1, Theorem 5.5]; again, we state it here merely for completeness and comparison with the exceptional case.

Theorem 7. (a) *Let $L \subset (L(p,1),\xi)$ be a Legendrian rational unknot in a tight contact structure on $L(p,1)$. Then $\mathtt{tb}_{\mathbb{Q}}(L) = n+1/p$ with n a negative integer, and $\mathtt{rot}_{\mathbb{Q}}(L)$ is of the form*

$$\mathtt{rot}_{\mathbb{Q}}(L) = r_0 + \frac{r_1}{p}$$

with

$$r_0 \in \{n+1, n+3, \ldots, -n-3, -n-1\}$$

and

$$r_1 \in \{-p+2, -p+4, \ldots, p-4, p-2\}.$$

Any such pair of invariants $(\mathtt{tb}_{\mathbb{Q}}, \mathtt{rot}_{\mathbb{Q}})$ is realised, and it determines L up to coarse equivalence, i.e. for each $n \leq -1$ we have $|n| \cdot (p-1)$ distinct Legendrian rational unknots.

(b) *Up to coarse equivalence, the exceptional rational unknots in an overtwisted $(L(p,1),\xi)$, $p \in \mathbb{N}$, are classified by their classical invariants $\mathtt{tb}_{\mathbb{Q}}$ and $\mathtt{rot}_{\mathbb{Q}}$. The possible values of $\mathtt{tb}_{\mathbb{Q}}$ are $n+1/p$ with $n \in \mathbb{N}_0$. For $n=0$, there is a single exceptional knot, and it has $\mathtt{rot}_{\mathbb{Q}} = 0$. For $n=1$, there are $p+1$ exceptional knots, with $\mathtt{rot}_{\mathbb{Q}}$ lying in the range*

$$\big\{-1, -1+\frac{2}{p}, -1+\frac{4}{p}, \ldots, -1+\frac{2p}{p} = +1\big\}.$$

For $n \geq 2$, there are $2p$ exceptional knots, with $\mathtt{rot}_{\mathbb{Q}}$ in the range

$$\big\{\pm\big(n-2+\frac{2}{p}\big), \pm\big(n-2+\frac{4}{p}\big), \ldots, \pm\big(n-2+\frac{2p}{p}\big) = \pm n\big\}.$$

Proof. Legendrian rational unknots in some tight contact structure on $L(p,1)$ can be found as follows. Take any tight $L(p,1)$ given by a surgery diagram as described after Proposition 4; this gives $p-1$ possibilities. Choose L to be a Legendrian unknot forming a Hopf link with the surgery curve, with $\mathtt{tb}_0 = n$ and $\mathtt{rot}_0$ in the range

$$\{n+1, n+3, \ldots, -n-3, -n-1\};$$

this gives us $|n|$ choices. With Lemma 2 one easily checks that the invariants of these examples are as listed in the theorem.

Examples of exceptional rational unknots whose invariants have the values stated in the theorem are shown in Figure 6.

The labels are to be understood as follows. For instance, in Figure 6(b) the surgery knot (and likewise L) has $k+1$ left-cusps on the left and $p+1-k$ right-cusps on the right, $k = 0, \ldots, p$. This means that $\mathtt{tb}_0 = -(p+1)$ and $\mathtt{rot}_0 = p-2k$ (for L oriented clockwise). In Figure 6(c) we take k in the range $1, \ldots, p$ and $n \geq 2$; using either orientation for L is going to give us the required $2p$ examples. Table 2 summarises the invariants of all exceptional examples. We defer the computations to Section 9.

In order to illustrate the range of methods available, we prove overtwistedness of the contact structures on $L(p,1)$ represented in Figure 6 by a different argument for each of the three diagrams.

For Figure 6(a) we appeal to the classification of tight contact structures on lens spaces [10, 13]. All these structures are Stein fillable. Now take $p-2$ additional parallel unknots and perform contact (-1)-surgery along them. This produces the diagram from Figure 4(a), and hence an overtwisted contact structure on $\mathbb{R}\mathrm{P}^3$. If the original surgery diagram had produced a tight (and hence, in this particular

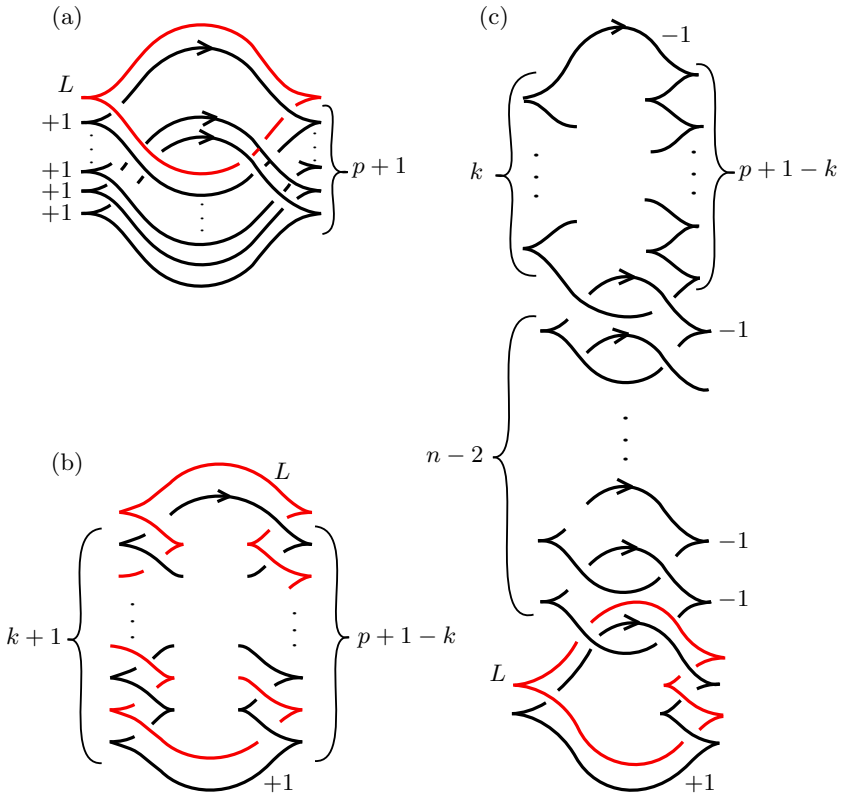

FIGURE 6. The exceptional rational unknots in $L(p,1)$.

Figure	n	k	$\mathtt{tb}_{\mathbb{Q}}(L)$	$\mathtt{rot}_{\mathbb{Q}}(L)$	$d_3(\xi)$
6(a)	-	-	$1/p$	0	$(3-p)/4$
6(b)	-	$0,\dots,p$	$1+\frac{1}{p}$	$-1+\frac{2k}{p}$	$-\frac{(p-2k)^2}{4p}+\frac{3}{4}$
6(c)	even ≥ 2	$1,\dots,p$	$n+\frac{1}{p}$	$\pm(n-2+\frac{2k}{p})$	$-\frac{(p-2k)^2}{4p}+\frac{3}{4}$
6(c)	odd ≥ 3	$1,\dots,p$	$n+\frac{1}{p}$	$\pm(n+\frac{2}{p}-\frac{2k}{p})$	$-\frac{(p-2k+2)^2}{4p}+\frac{3}{4}$

TABLE 2. Invariants of the exceptional rational unknots in $L(p,1)$.

case, Stein fillable) structure, the resulting structure on $\mathbb{R}\mathrm{P}^3$ would still be Stein fillable, and hence tight.

For Figure 6(b), we base our argument on the rational Bennequin inequality

$$\mathtt{tb}_{\mathbb{Q}}(L)+|\mathtt{rot}_{\mathbb{Q}}(L)|\leq -\frac{1}{r}\chi(\Sigma);$$

this inequality holds for any rationally null-homologous Legendrian knot of order r with rational Seifert surface Σ in any *tight* contact 3-manifold [1, Theorem 2.1]. Since the knot L in Figure 6(b) violates this inequality, the manifold given by that surgery diagram must be overtwisted.

In Figure 6(c) one may consider a Legendrian unknot with $\mathtt{tb} = -1$ and $\mathtt{rot} = 0$ forming a Hopf link with the 'shark' at the bottom of the picture. As in [5, Figure 2] one sees that this Legendrian unknot is the boundary of an overtwisted disc in the surgered manifold; the other surgery curves do not intersect this disc.

In each of the examples in Figure 6, L is exceptional by the same reasoning as in the case of $\mathbb{R}\mathrm{P}^3$ (in case (a) perform a $(-1/(p+1))$-surgery along L).

The argument that our list of examples is complete is very similar to the case of $\mathbb{R}\mathrm{P}^3$, and we only list a few of the necessary modifications. The gluing of V_1 and V_2 is now given by $\mu_2 = -\mu_1 + p\lambda_1$ and $\lambda_2 = \lambda_1$. With $\lambda_c = n\mu_1 + \lambda_1$, $n \in \mathbb{Z}$, we get $\mathtt{tb}_{\mathbb{Q}}(L) = n + 1/p$. The corresponding slope of ∂V_2 is $s_2 = -p - 1/n$.

For $n \leq -1$, there are $(p-1)\cdot|n|$ distinct contact structures on V_2. These correspond to the rational unknots in a tight $L(p,1)$.

For $n = 0$ there is again a unique tight contact structure on V_2. For $n \geq 1$, the slope $-p - 1/n$ has the continued fraction expansion $[-p-1, -2, \ldots, -2]$, where -2 occurs $n-1$ times. So we have $p+1$ tight structures for $n = 1$, and $2p$ each for $n \geq 2$. □

8. The lens space $L(5,2)$

We expect the analogue of Theorem 7 to hold for arbitrary lens spaces $L(p,q)$. The number of Legendrian realisations of the (at most) two rational unknots in $L(p,q)$ can be computed as before, and one can also develop some systematics in the surgery diagrams.

Instead of giving this general picture, we concentrate on one specific example, the lens space $L(5,2)$ and the two topological types K_1, K_2 of rational unknots described in Figure 2. This example serves to illustrate a 'stable' pattern in the surgery diagrams: for sufficiently large values of $\mathtt{tb}_{\mathbb{Q}}$, there is essentially one general diagram that covers all cases; for small values of $\mathtt{tb}_{\mathbb{Q}}$ one needs to find some *ad hoc* diagrams. The diagrams for the 'stable' situation generalise in a straightforward manner to $L(p,q)$.

For $L(5,2)$, the gluing map for the two Heegaard tori is given by $\mu_2 = -2\mu_1 + 5\lambda_1$ and $\lambda_2 = \mu_1 - 2\lambda_1$. For the contact framing $\lambda_c = n\mu_1 + \lambda_1$ of a Legendrian realisation of K_1 one then computes $\mathtt{tb}_{\mathbb{Q}} = n + 2/5$. The corresponding slope of the complementary solid torus V_2 is then equal to $(5n+2)/(2n+1)$, which after a single Dehn twist becomes

$$s_2' = -1 - \frac{2n+1}{3n+1} < -1.$$

In Table 3 we list the continued fraction expansions of this slope and the corresponding number of tight contact structures on V_2, which gives us the number of Legendrian realisations of K_1 with tight complements.

The cases with $n \leq -1$ correspond to a tight contact structure on $L(5,2)$ as follows. Realise $L(5,2)$ by contact (-1)-surgeries along a 'shark' and a standard $\mathtt{tb} = -1$ Legendrian unknot forming a Hopf link. A standard Legendrian unknot linked once with the shark gives a Legendrian realisation of K_1 with $\mathtt{tb}_{\mathbb{Q}} = -1 + 2/5$. Depending on a choice of orientation, this has $\mathtt{rot}_{\mathbb{Q}} = \pm 2/5$. By successive stabilisations of this knot, one obtains the $|2n|$ realisations with $\mathtt{tb}_{\mathbb{Q}} = n + 2/5$.

The surgery pictures of the exceptional realisations of K_1 are given in Figures 7 and 8; the invariants are listed in Table 4. The computations follow the same pattern as in the case of $L(p,1)$, so we shall not reproduce them here.

n	c.f.e. of s_2'	# Leg. real.
≤ -2	$[-2,-3,n]$	$\lvert 2n\rvert$
-1	$[-2,-2]$	2
0	-2	2
1	$[-2,-4]$	4
≥ 2	$[-2,-4,-2,\ldots,-2]$	6

TABLE 3. Number of Legendrian realisations of K_1 in $L(5,2)$.

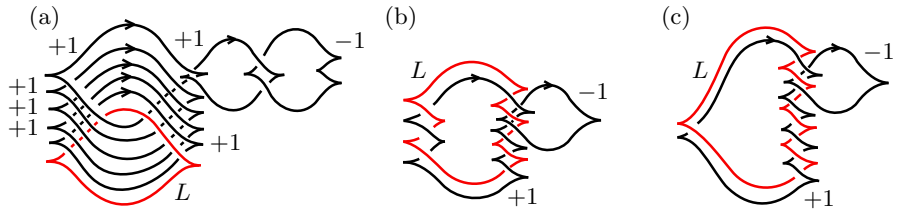

FIGURE 7. Exceptional rational unknots in $L(5,2)$ isotopic to K_1 I.

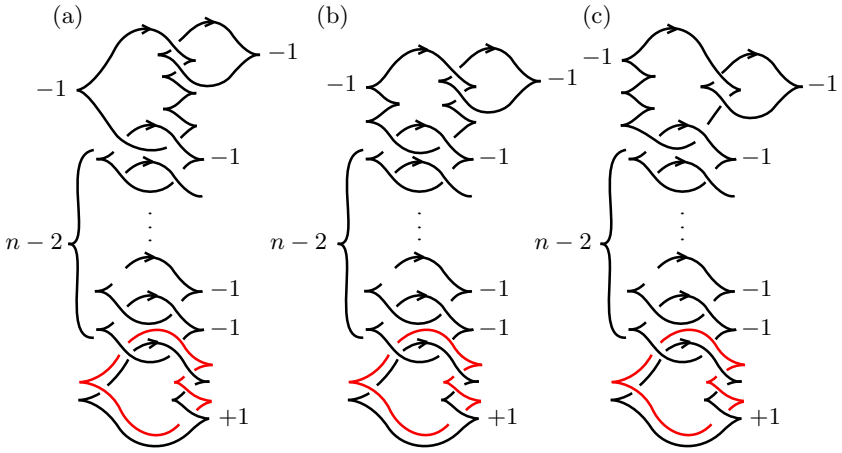

FIGURE 8. Exceptional rational unknots in $L(5,2)$ isotopic to K_1 II.

The Legendrian realisations of K_2 in $L(5,2)$ have $\mathtt{tb}_{\mathbb{Q}} = n+3/5$. The numbers of different realisations are listed in Table 5. Again, the cases with $n \leq -1$ correspond to a tight contact structure on $L(5,2)$, and they are realised in a similar fashion as the tight cases for K_1. For the exceptional realisations of K_2, see Figures 9 and 10 and Table 6.

9. SOME COMPUTATIONS

In this section we collect some hints for the computation of the invariants in various of the examples described above.

Figure	n	$\mathtt{tb}_{\mathbb{Q}}(L)$	$\mathtt{rot}_{\mathbb{Q}}(L)$
7(a)	-	$2/5$	$\pm 1/5$
7(b)	-	$7/5$	$\pm 2/5$
7(c)	-	$7/5$	$\pm 6/5$
8(a)	even ≥ 2	$n+2/5$	$\pm(n-7/5)$
8(a)	odd ≥ 3	$n+2/5$	$\pm(n+1/5)$
8(b)	≥ 2	$n+2/5$	$\pm(n-3/5)$
8(c)	even ≥ 2	$n+2/5$	$\pm(n+1/5)$
8(c)	odd ≥ 3	$n+2/5$	$\pm(n-7/5)$

TABLE 4. Invariants of the exceptional realisations of K_1 in $L(5,2)$.

n	c.f.e. of s_1'	# Leg. real.
≤ -2	$[-3,-2,n]$	$\lvert 2n\rvert$
-1	-2	2
0	-3	3
1	$[-3,-3]$	6
≥ 2	$[-3,-3,-2,\ldots,-2]$	8

TABLE 5. Number of Legendrian realisations of K_2 in $L(5,2)$.

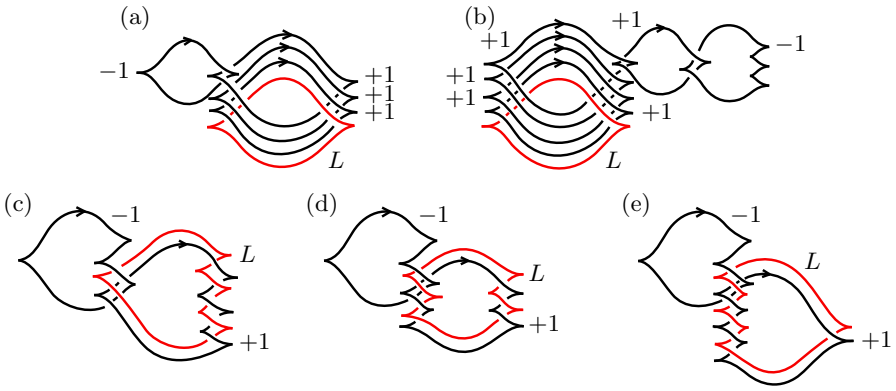

FIGURE 9. Exceptional rational unknots in $L(5,2)$ isotopic to K_2 I.

9.1. **Plamenevskaya's examples.** We consider the example in Figure 3(c). Here the linking matrix $M = M^{(n)}$ is the $((n-1)\times(n-1))$-matrix

$$M = \begin{pmatrix} -1 & -1 & & & & & \\ -1 & -2 & -1 & & & & \\ & -1 & -2 & -1 & & & \\ & & & \ddots & & & \\ & & & & \ddots & & \\ & & & & -1 & -2 & -1 \\ & & & & & -1 & -2 \end{pmatrix},$$

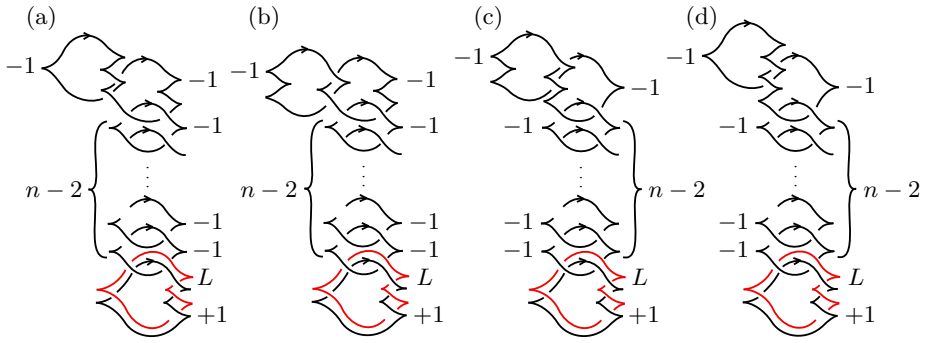

FIGURE 10. Exceptional rational unknots in $L(5,2)$ isotopic to K_2 II.

Figure	n	$\mathtt{tb}_{\mathbb{Q}}(L)$	$\mathtt{rot}_{\mathbb{Q}}(L)$
9(a)	-	$3/5$	0
9(b)	-	$3/5$	$\pm 2/5$
9(c)	-	$8/5$	$\pm 7/5$
9(d)	-	$8/5$	$\pm 1/5$
9(e)	-	$8/5$	± 1
10(a)	even ≥ 2	$n+3/5$	$\pm(n-6/5)$
10(a)	odd ≥ 3	$n+3/5$	$\pm(n+2/5)$
10(b)	even ≥ 2	$n+3/5$	$\pm(n-4/5)$
10(b)	odd ≥ 3	$n+3/5$	$\pm n$
10(c)	even ≥ 2	$n+3/5$	$\pm(n+2/5)$
10(c)	odd ≥ 3	$n+3/5$	$\pm(n-6/5)$
10(d)	even ≥ 2	$n+3/5$	$\pm n$
10(d)	odd ≥ 3	$n+3/5$	$\pm(n-4/5)$

TABLE 6. Invariants of the exceptional realisations of K_2 in $L(5,2)$.

where we have numbered the surgery curves $L_1,\dots,L_{n-1}$ from bottom to top in the figure. By successive subtraction of the i^{th} from the $(i+1)^{\text{st}}$ row, $i=1,\dots,n-2$, we obtain

$$\begin{pmatrix} -1 & -1 & & & & \\ 0 & -1 & -1 & & & \\ & 0 & -1 & -1 & & \\ & & & \ddots & & \\ & & & & -1 & -1 \\ & & & & 0 & -1 \end{pmatrix},$$

hence $\det M = (-1)^{n-1}$. The first row of M^{-1} is

$$(-(n-1), n-2, -(n-3), \dots, (-1)^{n-1}\cdot 1).$$

This information suffices to compute the rotation number of L (with clockwise orientation):

$$\mathtt{rot}(L) = 1 - \left\langle \begin{pmatrix} 1 \\ 0 \\ 0 \\ \vdots \\ 0 \end{pmatrix}, M^{-1} \begin{pmatrix} -2 \\ -1 \\ 0 \\ \vdots \\ 0 \end{pmatrix} \right\rangle = 1 - 2(n-1) + n - 2 = -(n-1).$$

By successive subtraction of the i^{th} from the $(i+1)^{\text{st}}$ row, starting from $i = 2$, in the $(n \times n)$-matrix $M_0^{(n)}$ we obtain

$$\begin{pmatrix} 0 & -2 & -1 & & & & \\ -2 & -1 & -1 & & & & \\ 1 & 0 & -1 & -1 & & & \\ -1 & 0 & 0 & -1 & -1 & & \\ \vdots & & & & \ddots & & \\ (-1)^{n-2} & & & & & -1 & -1 \\ (-1)^{n-1} & & & & & 0 & -1 \end{pmatrix}.$$

By expanding the determinant of this matrix along the last row one shows inductively that

$$\det M_0^{(n)} = (-1)^{n-1}(n+2).$$

Hence

$$\mathtt{tb}(L) = -2 + \frac{(-1)^{n-1}(n+2)}{(-1)^{n-1}} = n.$$

9.2. **Projective 3-space.** We consider the example in Figure 5(a). The Kirby moves that transform the surgery link into a single unknot with topological framing -2, and L into the rational unknot of Figure 1, are shown in Figure 11. These moves are analogous to those in Plamenevskaya's example [17, Figure 4]; we say more about them further down, where we use them to compute $\mathtt{tb}_{\mathbb{Q}}(L)$ without appealing to Lemma 2.

The linking matrix $M = M^{(n)}$ is the $(n \times n)$-matrix

$$M = \begin{pmatrix} -1 & -1 & & & & & \\ -1 & -2 & -1 & & & & \\ & -1 & -2 & -1 & & & \\ & & & \ddots & & & \\ & & & & \ddots & & \\ & & & & -1 & -2 & -1 \\ & & & & & -1 & -3 \end{pmatrix},$$

where, as before, we have numbered the surgery curves $L_1, \dots, L_n$ from bottom to top. Observe that this $M^{(n)}$ equals the $M^{(n+1)}$ from the previous example, with a single change in the very last entry of the matrix. Hence, arguing as before, one obtains $\det M = (-1)^n \cdot 2$.

The first row of M^{-1} is

$$(-(2n-1)/2, (2n-3)/2, -(2n-5)/2, \dots, (-1)^n/2); \tag{5}$$

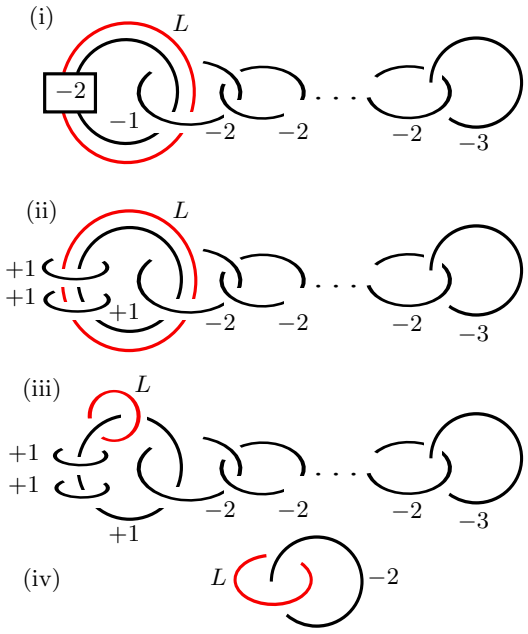

FIGURE 11. Kirby moves for the example in Figure 5(a).

the last row is

$$((-1)^n/2, (-1)^{n-1}/2, \dots, 1/2, -1/2). \tag{6}$$

Hence, with L oriented clockwise,

$$\begin{aligned}
\mathtt{rot}_{\mathbb{Q}}(L) &= 1 - \left\langle \begin{pmatrix} 1 \\ 0 \\ \vdots \\ 0 \\ 1 \end{pmatrix}, M^{-1} \begin{pmatrix} -2 \\ -1 \\ 0 \\ \vdots \\ 0 \end{pmatrix} \right\rangle \\
&= 1 - (2n - 1 - \frac{2n-3}{2} + (-1)^{n-1} - (-1)^{n-1} \cdot \frac{1}{2}) \\
&= -n + \frac{1}{2} + (-1)^n \cdot \frac{1}{2} \\
&= \begin{cases} -(n-1) & \text{for } n \text{ even}, \\ -n & \text{for } n \text{ odd}. \end{cases}
\end{aligned}$$

By expanding the determinant of $M_0^{(n)}$, transformed as in the previous example, along the last row, and using the result from the previous example, one obtains

$$\det M_0^{(n)} = (-1)^n(2n+5).$$

Hence

$$\mathtt{tb}_{\mathbb{Q}}(L) = -2 + \frac{(-1)^n(2n+5)}{(-1)^n \cdot 2} = n + \frac{1}{2}.$$

Alternatively, $\mathtt{tb}_{\mathbb{Q}}(L)$ can be computed by keeping track of the framing of L during the Kirby moves in Figure 11. In S^3 we have $\mathtt{tb}(L) = -2$, so initially the contact

framing of L is given by $-2\mu_0 + \lambda_0$, where λ_0 is (and remains throughout the following moves) the longitude corresponding to the surface framing in S^3. This framing curve can be thought of as a parallel copy of L, also going through the (-2)-box.

To get from (i) to (ii), we make two positive blow-ups, i.e. we add two $(+1)$-framed unknots to the picture (corresponding to taking the connected sum with two copies of $\mathbb{C}\mathrm{P}^2$), and then slide L and the (-1)-framed knot over them to undo the (-2)-linking. This adds two positive twists to the framing of L, so the framing is now λ_0.

To get from (ii) to (iii), we slide L over the parallel $(+1)$-framed unknot. This adds $+1$ to the framing of L. To get from (iii) to (iv), we first blow down the two $(+1)$-framed unknots not linked with L. This has no effect on L, but changes the third $(+1)$-framed unknot into a (-1)-framed one. Now we blow down the chain of unknots, starting with the (-1)-framed one. At each step, the adjacent (-2)-framed unknot gets framing -1, and the framing of L increases by 1. Since we have to blow down a total of $n-1$ (-1)-framed unknots to obtain (iv), the framing of L finally becomes $n\mu_0 + \lambda_0$.

Now recall equation (3) from the proof of Lemma 2 and the argument preceding it. The unique $a_0 \in \mathbb{Z}$ such that $a_0\mu_0 + 2\lambda_0$ is nullhomologous in the surgered manifold given by Figure 11(iv) is $a_0 = -1$. Hence

$$2 \cdot \mathtt{tb}_{\mathbb{Q}}(L) = (n\mu_0 + \lambda_0) \bullet (-\mu_0 + 2\lambda_0) = 2n + 1,$$

giving us the same result for $\mathtt{tb}_{\mathbb{Q}}(L)$ as before.

Here is how to compute $d_3(\xi)$ for this example. The surgery diagram is equivalent to $n-1$ unlinked (-1)-framed unknots and a further unlinked (-2)-framed unknot. So the signature of the 4-dimensional filling X is $-n$, its Euler characteristic is $n+1$. In order to compute c^2, we follow the algorithm described in [5]. The Poincaré dual $\mathrm{PD}(c) \in H_2(X, \partial X)$ — in terms of the obvious generators of $H_2(X, \partial X)$, the meridional discs to the surgery curves — is given by the vector $(1, 0, \ldots, 0, 1)$ of rotation numbers. The homomorphism $H_2(X) \to H_2(X, \partial X)$ induced by inclusion is described, again in terms of the obvious bases, by the linking matrix M, so the class $C \in H_2(X)$ that maps to $\mathrm{PD}(c)$ can be thought of as a row vector with $MC^t = (1, 0, \ldots, 0, 1)^t$. So this vector C is given by the sum of the vectors in (5) and (6). Then

$$\begin{aligned} c^2 &= C^2 = CMC^t \\ &= C \cdot (1, 0, \ldots, 0, 1)^t \\ &= -\frac{2n-1}{2} + \frac{(-1)^n}{2} + \frac{(-1)^n}{2} - \frac{1}{2} \\ &= -n + (-1)^n. \end{aligned}$$

Then with equation (4), observing that $q = 1$ in this example, we obtain

$$d_3(\xi) = \begin{cases} 3/4 & \text{for } n \text{ even}, \\ 1/4 & \text{for } n \text{ odd}. \end{cases}$$

9.3. **The lens spaces $L(p, 1)$.** We start with the example in Figure 6(a). The Kirby moves in Figure 12 show that L is the rational unknot in $L(p, 1)$.

The linking matrix is the $((p+1) \times (p+1))$-matrix M with zeros on the diagonal and all other entries equal to 1. It is a simple exercise to show that $\det M = -p$.

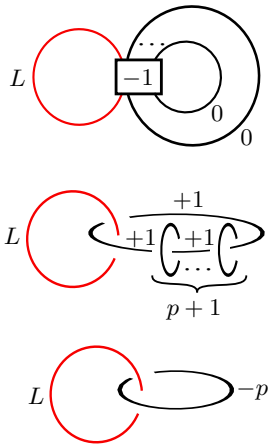

FIGURE 12. Kirby moves for the example in Figure 6(a).

Correspondingly, $\det M_0 = -(p+1)$. It follows that

$$\mathtt{tb}_{\mathbb{Q}}(L) = -1 + \frac{p+1}{p} = \frac{1}{p}.$$

Since $\mathtt{rot}_0, \mathtt{rot}_1, \ldots, \mathtt{rot}_{p+1} = 0$, we have $\mathtt{rot}_{\mathbb{Q}}(L) = 0$.

Next we consider the example in Figure 6(b). Here the topological Kirby diagram shows directly that L is the rational unknot in $L(p,1)$. The linking matrix M is the (1×1)-matrix $(-p)$, the matrix M_0 is

$$\begin{pmatrix} 0 & -(p+1) \\ -(p+1) & -p \end{pmatrix}.$$

Hence

$$\mathtt{tb}_{\mathbb{Q}}(L) = -(p+1) + \frac{(p+1)^2}{p} = 1 + \frac{1}{p}.$$

The rotation numbers $\mathtt{rot}_i$, $i = 0, 1$, equal $p - 2k$ (with L oriented clockwise). Hence

$$\mathtt{rot}_{\mathbb{Q}}(L) = p - 2k - (p-2k)\cdot\big(-\frac{1}{p}\big)\cdot\big(-(p+1)\big) = -1 + \frac{2k}{p}.$$

So for k in the range $0, \ldots, p$ we get $p+1$ different Legendrian realisations.

Finally, we come to the example in Figure 6(c). Here the computations are minor modifications of those for the example we discussed in the case of $\mathbb{R}\mathrm{P}^3$. The Kirby moves for showing that L is the rational unknot are as in Figure 11. The linking matrix M differs from the one in that previous case by the substitution of $-(p+1)$ for -3. Thus, one finds $\det M = (-1)^n \cdot p$ and $\det M_0 = (-1)^n\big(p(n+2)+1\big)$, which yields

$$\mathtt{tb}_{\mathbb{Q}}(L) = n + \frac{1}{p}.$$

The first row of M^{-1} is now

$$\big(-\frac{(n-1)p+1}{p}, \frac{(n-2)p+1}{p}, \ldots, (-1)^{n-1}\frac{p+1}{p}, (-1)^n\frac{1}{p}\big);$$

the last row is

$$((-1)^n/p, (-1)^{n-1}/p, \dots, 1/p, -1/p).$$

With the rotation number of the surgery curve at the top of Figure 6(c) being $\mathtt{rot}_n = p-2k+1$, one computes with Lemma 2 that $\mathtt{rot}_{\mathbb{Q}}(L)$, with either orientation of L, takes for $k = 1, \dots, p$ the values claimed in Theorem 7.

We close with some comments about the computation of the d_3-invariant. For the example in Figure 6(a), the only term in formula (4) that is not entirely obvious is the signature. Topologically, the surgery diagram consists of $p+1$ 0-framed unknots with a common (-1)-linking. By making a $(+1)$-blow up and sliding the corresponding $(+1)$-framed unknot over this link, we obtain $p+1$ unlinked $(+1)$-framed unknots, all of which are linked once with the extra $(+1)$-framed unknot. By sliding the $p+1$ unknots off the extra one, we obtain an unlink consisting of a single $(-p)$-framed unknot and $p+1$ $(+1)$-framed unknots. This describes a filling of signature p. Since we had to add a $(+1)$-framed unknot to arrive at this picture, we have $\sigma = p-1$.

The computation of d_3 for the example in Figure 6(b) presents no difficulty.

For the example in Figure 6(c), one sees $\sigma = -n$ by an argument similar to that for (a). Since the surgery diagram corresponds to adding n 2-handles, we have $\chi = 1+n$. The vector of rotation numbers is given by $(1, 0, \dots, 0, p-2k+1)$, i.e. we need to solve the equation

$$MC^t = (1, 0, \dots, 0, p-2k+1)^t$$

over $\mathbb{Q}$. This is achieved by

$$C = \begin{cases} \frac{1}{p}\big(-(2k+(n-2)p), +(2k+(n-3)p), \dots, -2k, +(2k-p)\big) & \text{for } n \text{ even}, \\ \frac{1}{p}\big(+(2k-np-2), \dots, -(2k-2p-2), +(2k-p-2)\big) & \text{for } n \text{ odd}. \end{cases}$$

Then one computes as in Section 9.2.

Acknowledgements. A major part of the work on this project was done during an inspiring "Research in Pairs" stay at the Mathematisches Forschungsinstitut Oberwolfach in September 2012. We thank the Forschungsinstitut for its support, and its efficient and friendly staff for creating an exceptional research environment.

References

[1] K. L. Baker and J. B. Etnyre, Rational linking and contact geometry, *Perspectives in Analysis, Geometry, and Topology*, Progr. Math. **296** (Birkhäuser, Basel, 2012), 19–37.
[2] K. L. Baker and J. E. Grigsby, Grid diagrams and Legendrian lens space links, *J. Symplectic Geom.* **7** (2009), 415–448.
[3] F. Bonahon, Difféotopies des espaces lenticulaires, *Topology* **22** (1983), 305–314.
[4] F. Ding and H. Geiges, A Legendrian surgery presentation of contact 3-manifolds, *Math. Proc. Cambridge Philos. Soc.* **136** (2004), 583–598.
[5] F. Ding, H. Geiges and A. I. Stipsicz, Surgery diagrams for contact 3-manifolds, *Turkish J. Math.* **28** (2004), 41–74.
[6] Ya. Eliashberg, Classification of overtwisted contact structures on 3-manifolds, *Invent. Math.* **98** (1989), 623–637.
[7] Ya. Eliashberg and M. Fraser, Topologically trivial Legendrian knots, *J. Symplectic Geom.* **7** (2009), 77–127.
[8] J. B. Etnyre, On knots in overtwisted contact structures, *Quantum Topol.*, to appear.
[9] H. Geiges, *An Introduction to Contact Topology*, Cambridge Stud. Adv. Math. **109** (Cambridge University Press, Cambridge, 2008).
[10] E. Giroux, Structures de contact en dimension trois et bifurcations des feuilletages de surfaces, *Invent. Math.* **141** (2000), 615–689.

[11] R. E. Gompf, Handlebody construction of Stein surfaces, *Ann. of Math. (2)* **148** (1998), 619–693.
[12] R. E. Gompf and A. I. Stipsicz, 4-*Manifolds and Kirby Calculus*, Grad. Stud. Math. **20** (American Mathematical Society, Providence, RI, 1999).
[13] K. Honda, On the classification of tight contact structures I, *Geom. Topol.* **4** (2000), 309–368.
[14] P. Lisca, P. Ozsváth, A. I. Stipsicz and Z. Szabó, Heegaard Floer invariants of Legendrian knots in contact three-manifolds, *J. Eur. Math. Soc. (JEMS)* **11** (2009), 1307–1363.
[15] D. McCullough, Isometries of elliptic 3-manifolds, *J. London Math. Soc. (2)* **65** (2002), 167–182.
[16] F. Öztürk, Generalised Thurston–Bennequin invariants for real algebraic surface singularities, *Manuscripta Math.* **117** (2005), 273–298.
[17] O. Plamenevskaya, On Legendrian surgeries between lens spaces, *J. Symplectic Geom.* **10** (2012), 165–181.

Mathematisches Institut, Universität zu Köln, Weyertal 86–90, 50931 Köln, Germany
E-mail address: geiges@math.uni-koeln.de

Department of Mathematics, Hacettepe University, 06800 Beytepe-Ankara, Turkey
E-mail address: sonaran@hacettepe.edu.tr